

Study of the Semileptonic Decay $\Lambda_c^+ \rightarrow \Lambda e^+ \nu_e$

- M. Ablikim¹, M. N. Achasov^{11,b}, P. Adlarson⁷⁰, M. Albrecht⁴, R. Aliberti³¹, A. Amoroso^{69A,69C}, M. R. An³⁵, Q. An^{66,53}, X. H. Bai⁶¹, Y. Bai⁵², O. Bakina³², R. Baldini Ferroli^{26A}, I. Balossino^{1,27A}, Y. Ban^{42,g}, V. Batozskaya^{1,40}, D. Becker³¹, K. Begzsuren²⁹, N. Berger³¹, M. Bertani^{26A}, D. Bettoni^{27A}, F. Bianchi^{69A,69C}, J. Bloms⁶³, A. Bortone^{69A,69C}, I. Boyko³², R. A. Briere⁵, A. Brueggemann⁶³, H. Cai⁷¹, X. Cai^{1,53}, A. Calcaterra^{26A}, G. F. Cao^{1,58}, N. Cao^{1,58}, S. A. Cetin^{57A}, J. F. Chang^{1,53}, W. L. Chang^{1,58}, G. Chelkov^{32,a}, C. Chen³⁹, Chao Chen⁵⁰, G. Chen¹, H. S. Chen^{1,58}, M. L. Chen^{1,53}, S. J. Chen³⁸, S. M. Chen⁵⁶, T. Chen¹, X. R. Chen^{28,58}, X. T. Chen¹, Y. B. Chen^{1,53}, Z. J. Chen^{23,h}, W. S. Cheng^{69C}, S. K. Choi⁵⁰, X. Chu³⁹, G. Cibinetto^{27A}, F. Cossio^{69C}, J. J. Cui⁴⁵, H. L. Dai^{1,53}, J. P. Dai⁷³, A. Dbeysi¹⁷, R. E. de Boer⁴, D. Dedovich³², Z. Y. Deng¹, A. Denig³¹, I. Denysenko³², M. Destefanis^{69A,69C}, F. De Mori^{69A,69C}, Y. Ding³⁶, J. Dong^{1,53}, L. Y. Dong^{1,58}, M. Y. Dong^{1,53,58}, X. Dong⁷¹, S. X. Du⁷⁵, P. Egorov^{32,a}, Y. L. Fan⁷¹, J. Fang^{1,53}, S. S. Fang^{1,58}, W. X. Fang¹, Y. Fang¹, R. Farinelli^{27A}, L. Fava^{69B,69C}, F. Feldbauer⁴, G. Felici^{26A}, C. Q. Feng^{66,53}, J. H. Feng⁵⁴, K. Fischer⁶⁴, M. Fritsch⁴, C. Fritzsch⁶³, C. D. Fu¹, H. Gao⁵⁸, Y. N. Gao^{42,g}, Yang Gao^{66,53}, S. Garbolino^{69C}, I. Garzia^{27A,27B}, P. T. Ge⁷¹, Z. W. Ge³⁸, C. Geng⁵⁴, E. M. Gersabeck⁶², A. Gilman⁶⁴, K. Goetzen¹², L. Gong³⁶, W. X. Gong^{1,53}, W. Gradl³¹, M. Greco^{69A,69C}, L. M. Gu³⁸, M. H. Gu^{1,53}, Y. T. Gu¹⁴, C. Y. Guan^{1,58}, A. Q. Guo^{28,58}, L. B. Guo³⁷, R. P. Guo⁴⁴, Y. P. Guo^{10,f}, A. Guskov^{32,a}, T. T. Han⁴⁵, W. Y. Han³⁵, X. Q. Hao¹⁸, F. A. Harris⁶⁰, K. K. He⁵⁰, K. L. He^{1,58}, F. H. Heinsius⁴, C. H. Heinz³¹, Y. K. Heng^{1,53,58}, C. Herold⁵⁵, M. Himmelreich^{12,d}, G. Y. Hou^{1,58}, Y. R. Hou⁵⁸, Z. L. Hou¹, H. M. Hu^{1,58}, J. F. Hu^{51,i}, T. Hu^{1,53,58}, Y. Hu¹, G. S. Huang^{66,53}, K. X. Huang⁵⁴, L. Q. Huang⁶⁷, L. Q. Huang^{28,58}, X. T. Huang⁴⁵, Y. P. Huang¹, Z. Huang^{42,g}, T. Hussain⁶⁸, N. Hüskens^{25,31}, W. Imoehl²⁵, M. Irshad^{66,53}, J. Jackson²⁵, S. Jaeger⁴, S. Janchiv²⁹, E. Jang⁵⁰, J. H. Jeong⁵⁰, Q. Ji¹, Q. P. Ji¹⁸, X. B. Ji^{1,58}, X. L. Ji^{1,53}, Y. Y. Ji⁴⁵, Z. K. Jia^{66,53}, H. B. Jiang⁴⁵, S. S. Jiang³⁵, X. S. Jiang^{1,53,58}, Y. Jiang⁵⁸, J. B. Jiao⁴⁵, Z. Jiao²¹, S. Jin³⁸, Y. Jin⁶¹, M. Q. Jing^{1,58}, T. Johansson⁷⁰, N. Kalantar-Nayestanaki⁵⁹, X. S. Kang³⁶, R. Kappert⁵⁹, M. Kavatsyuk⁵⁹, B. C. Ke⁷⁵, I. K. Keshk⁴, A. Khokhaz⁶³, P. Kiese³¹, R. Kiuchi¹, R. Kliemt¹², L. Koch³³, O. B. Kolcu^{57A}, B. Kopf⁴, M. Kuemmel⁴, M. Kuessner⁴, A. Kupsc^{40,70}, W. Kühn³³, J. J. Lane⁶², J. S. Lange³³, P. Larin¹⁷, A. Lavania²⁴, L. Lavezzi^{69A,69C}, Z. H. Lei^{66,53}, H. Leithoff³¹, M. Lellmann³¹, T. Lenz³¹, C. Li⁴³, C. Li³⁹, C. H. Li³⁵, Cheng Li^{66,53}, D. M. Li⁷⁵, F. Li^{1,53}, G. Li¹, H. Li⁴⁷, H. Li^{66,53}, H. B. Li^{1,58}, H. J. Li¹⁸, H. N. Li^{51,i}, J. Q. Li⁴, J. S. Li⁵⁴, J. W. Li⁴⁵, Ke Li¹, L. J. Li¹, L. K. Li¹, Lei Li³, M. H. Li³⁹, P. R. Li^{34,j,k}, S. X. Li¹⁰, S. Y. Li⁵⁶, T. Li⁴⁵, W. D. Li^{1,58}, W. G. Li¹, X. H. Li^{66,53}, X. L. Li⁴⁵, Xiaoyu Li^{1,58}, H. Liang^{66,53}, H. Liang^{1,58}, H. Liang³⁰, Y. F. Liang⁴⁹, Y. T. Liang^{28,58}, G. R. Liao¹³, L. Z. Liao⁴⁵, J. Libby²⁴, A. Limphirat⁵⁵, C. X. Lin⁵⁴, D. X. Lin^{28,58}, T. Lin¹, B. J. Liu¹, C. X. Liu¹, D. Liu^{17,66}, F. H. Liu⁴⁸, Fang Liu¹, Feng Liu⁶, G. M. Liu^{51,i}, H. Liu^{34,j,k}, H. B. Liu¹⁴, H. M. Liu^{1,58}, Huanhuan Liu¹, Huihui Liu¹⁹, J. B. Liu^{66,53}, J. L. Liu⁶⁷, J. Y. Liu^{1,58}, K. Liu¹, K. Y. Liu³⁶, Ke Liu²⁰, L. Liu^{66,53}, M. H. Liu^{10,f}, P. L. Liu¹, Q. Liu⁵⁸, S. B. Liu^{66,53}, T. Liu^{10,f}, W. K. Liu³⁹, W. M. Liu^{66,53}, X. Liu^{34,j,k}, Y. Liu^{34,j,k}, Y. B. Liu³⁹, Z. A. Liu^{1,53,58}, Z. Q. Liu⁴⁵, X. C. Lou^{1,53,58}, F. X. Lu⁵⁴, H. J. Lu²¹, J. G. Lu^{1,53}, X. L. Lu¹, Y. Lu⁷, Y. P. Lu^{1,53}, Z. H. Lu¹, C. L. Luo³⁷, M. X. Luo⁷⁴, T. Luo^{10,f}, X. L. Luo^{1,53}, X. R. Lyu⁵⁸, Y. F. Lyu³⁹, F. C. Ma³⁶, H. L. Ma¹, L. L. Ma⁴⁵, M. M. Ma^{1,58}, Q. M. Ma¹, R. Q. Ma^{1,58}, R. T. Ma⁵⁸, X. Y. Ma^{1,53}, Y. Ma^{42,g}, F. E. Maas¹⁷, M. Maggiora^{69A,69C}, S. Maldaner⁴, S. Malde⁶⁴, Q. A. Malik⁶⁸, A. Mangoni^{26B}, Y. J. Mao^{42,g}, Z. P. Mao¹, S. Marcello^{69A,69C}, Z. X. Meng⁶¹, J. G. Messchendorp^{59,12}, G. Mezzadri^{1,27A}, H. Miao¹, T. J. Min³⁸, R. E. Mitchell²⁵, X. H. Mo^{1,53,58}, N. Yu. Muchnoi^{11,b}, Y. Nefedov³², F. Nerling^{17,d}, I. B. Nikolaev¹¹, Z. Ning^{1,53}, S. Nisar^{9,l}, Y. Niu⁴⁵, S. L. Olsen⁵⁸, Q. Ouyang^{1,53,58}, S. Pacetti^{26B,26C}, X. Pan^{10,f}, Y. Pan⁵², A. Pathak³⁰, M. Pelizaeus⁴, H. P. Peng^{66,53}, K. Peters^{12,d}, J. Pettersson⁷⁰, J. L. Ping³⁷, R. G. Ping^{1,58}, S. Plura³¹, S. Pogodin³², V. Prasad^{66,53}, F. Z. Qi¹, H. Qi^{66,53}, H. R. Qi⁵⁶, M. Qi³⁸, T. Y. Qi^{10,f}, S. Qian^{1,53}, W. B. Qian⁵⁸, Z. Qian⁵⁴, C. F. Qiao⁵⁸, J. J. Qin⁶⁷, L. Q. Qin¹³, X. P. Qin^{10,f}, X. S. Qin⁴⁵, Z. H. Qin^{1,53}, J. F. Qiu¹, S. Q. Qu⁵⁶, K. H. Rashid⁶⁸, C. F. Redmer³¹, K. J. Ren³⁵, A. Rivetti^{69C}, V. Rodin⁵⁹, M. Rolo^{69C}, G. Rong^{1,58}, Ch. Rosner¹⁷, S. N. Ruan³⁹, H. S. Sang⁶⁶, A. Sarantsev^{32,c}, Y. Schelhaas³¹, C. Schnier⁴, K. Schönnung⁷⁰, M. Scodello^{27A,27B}, K. Y. Shan^{10,f}, W. Shan²², X. Y. Shan^{66,53}, J. F. Shangguan⁵⁰, L. G. Shao^{1,58}, M. Shao^{66,53}, C. P. Shen^{10,f}, H. F. Shen^{1,58}, X. Y. Shen^{1,58}, B.-A. Shi⁵⁸, H. C. Shi^{66,53}, J. Y. Shi¹, Q. Q. Shi⁵⁰, R. S. Shi^{1,58}, X. Shi^{1,53}, X. D. Shi^{66,53}, J. J. Song¹⁸, W. M. Song^{1,30}, Y. X. Song^{42,g}, S. Sosio^{69A,69C}, S. Spataro^{69A,69C}, F. Stieler³¹, K. X. Su⁷¹, P. P. Su⁵⁰, Y.-J. Su⁵⁸, G. X. Sun¹, H. Sun⁵⁸, H. K. Sun¹, J. F. Sun¹⁸, L. Sun⁷¹, S. S. Sun^{1,58}, T. Sun^{1,58}, W. Y. Sun³⁰, X. Sun^{23,h}, Y. J. Sun^{66,53}, Y. Z. Sun¹, Z. T. Sun⁴⁵, Y. H. Tan⁷¹, Y. X. Tan^{66,53}, C. J. Tang⁴⁹, G. Y. Tang¹, J. Tang⁵⁴, L. Y. Tao⁶⁷, Q. T. Tao^{23,h}, M. Tat⁶⁴, J. X. Teng^{66,53}, V. Thoren⁷⁰, W. H. Tian⁴⁷, Y. Tian^{28,58}, I. Uman^{57B}, B. Wang¹, B. L. Wang⁵⁸, C. W. Wang³⁸, D. Y. Wang^{42,g}, F. Wang⁶⁷, H. J. Wang^{34,j,k}, H. P. Wang^{1,58}, K. Wang^{1,53}, L. L. Wang¹, M. Wang⁴⁵, M. Z. Wang^{42,g}, Meng Wang^{1,58}, S. Wang^{10,f}, T. Wang^{10,f}, T. J. Wang³⁹, W. Wang⁵⁴, W. H. Wang⁷¹, W. P. Wang^{66,53}, X. Wang^{42,g}, X. F. Wang^{34,j,k}, X. L. Wang^{10,f}, Y. Wang⁵⁶, Y. D. Wang⁴¹, Y. F. Wang^{1,53,58}, Y. H. Wang⁴³, Y. Q. Wang¹, Yaqian Wang^{1,16}, Z. Wang^{1,53}, Z. Y. Wang^{1,58}, Ziyi Wang⁵⁸, D. H. Wei¹³, F. Weidner⁶³, S. P. Wen¹, D. J. White⁶², U. Wiedner⁴, G. Wilkinson⁶⁴, M. Wolke⁷⁰, L. Wollenberg⁴, J. F. Wu^{1,58}, L. H. Wu¹, L. J. Wu^{1,58}, X. Wu^{10,f}, X. H. Wu³⁰, Y. Wu⁶⁶, Z. Wu^{1,53}, L. Xia^{66,53}, T. Xiang^{42,g}, D. Xiao^{34,j,k}, G. Y. Xiao³⁸, H. Xiao^{10,f}, S. Y. Xiao¹, Y. L. Xiao^{10,f}, Z. J. Xiao³⁷, C. Xie³⁸, X. H. Xie^{42,g}, Y. Xie⁴⁵, Y. G. Xie^{1,53}, Y. H. Xie⁶, Z. P. Xie^{66,53}, T. Y. Xing^{1,58}, C. F. Xu¹, C. J. Xu⁵⁴, G. F. Xu¹, H. Y. Xu⁶¹, Q. J. Xu¹⁵, S. Y. Xu⁶⁵, X. P. Xu⁵⁰, Y. C. Xu⁵⁸, Z. P. Xu³⁸, F. Yan^{10,f}, L. Yan^{10,f}, W. B. Yan^{66,53}, W. C. Yan⁷⁵, H. J. Yang^{46,e}, H. L. Yang³⁰, H. X. Yang¹, L. Yang⁴⁷, S. L. Yang⁵⁸, Tao Yang¹, Y. X. Yang^{1,58}, Yifan Yang^{1,58}, M. Ye^{1,53}, M. H. Ye⁸, J. H. Yin¹, Z. Y. You⁵⁴, B. X. Yu^{1,53,58}, C. X. Yu³⁹, G. Yu^{1,58}, T. Yu⁶⁷, C. Z. Yuan^{1,58}, L. Yuan², S. C. Yuan¹, X. Q. Yuan¹, Y. Yuan^{1,58}, Z. Y. Yuan⁵⁴, C. X. Yue³⁵, A. A. Zafar⁶⁸, F. R. Zeng⁴⁵, X. Zeng⁶, Y. Zeng^{23,h}, Y. H. Zhan⁵⁴, A. Q. Zhang¹, B. L. Zhang¹, B. X. Zhang¹, D. H. Zhang³⁹, G. Y. Zhang¹⁸, H. Zhang⁶⁶, H. H. Zhang⁵⁴, H. H. Zhang³⁰, H. Y. Zhang^{1,53}, J. L. Zhang⁷², J. Q. Zhang³⁷, J. W. Zhang^{1,53,58}, J. X. Zhang^{34,j,k}, J. Y. Zhang¹, J. Z. Zhang^{1,58}, Jianyu Zhang^{1,58}, Jiawei Zhang^{1,58}, L. M. Zhang⁵⁶, L. Q. Zhang⁵⁴, Lei Zhang³⁸, P. Zhang¹, Q. Y. Zhang^{35,75},

Shulei Zhang^{23,h}, X. D. Zhang⁴¹, X. M. Zhang¹, X. Y. Zhang⁴⁵, X. Y. Zhang⁵⁰, Y. Zhang⁶⁴, Y. T. Zhang⁷⁵, Y. H. Zhang^{1,53}, Yan Zhang^{66,53}, Yao Zhang¹, Z. H. Zhang¹, Z. Y. Zhang⁷¹, Z. Y. Zhang³⁹, G. Zhao¹, J. Zhao³⁵, J. Y. Zhao^{1,58}, J. Z. Zhao^{1,53}, Lei Zhao^{66,53}, Ling Zhao¹, M. G. Zhao³⁹, Q. Zhao¹, S. J. Zhao⁷⁵, Y. B. Zhao^{1,53}, Y. X. Zhao^{28,58}, Z. G. Zhao^{66,53}, A. Zhemchugov^{32,a}, B. Zheng⁶⁷, J. P. Zheng^{1,53}, Y. H. Zheng⁵⁸, B. Zhong³⁷, C. Zhong⁶⁷, X. Zhong⁵⁴, H. Zhou⁴⁵, L. P. Zhou^{1,58}, X. Zhou⁷¹, X. K. Zhou⁵⁸, X. R. Zhou^{66,53}, X. Y. Zhou³⁵, Y. Z. Zhou^{10,f}, J. Zhu³⁹, K. Zhu¹, K. J. Zhu^{1,53,58}, L. X. Zhu⁵⁸, S. H. Zhu⁶⁵, S. Q. Zhu³⁸, T. J. Zhu⁷², W. J. Zhu^{10,f}, Y. C. Zhu^{66,53}, Z. A. Zhu^{1,58}, B. S. Zou¹, J. H. Zou¹

(BESIII Collaboration)

¹ Institute of High Energy Physics, Beijing 100049, People's Republic of China

² Beihang University, Beijing 100191, People's Republic of China

³ Beijing Institute of Petrochemical Technology, Beijing 102617, People's Republic of China

⁴ Bochum Ruhr-University, D-44780 Bochum, Germany

⁵ Carnegie Mellon University, Pittsburgh, Pennsylvania 15213, USA

⁶ Central China Normal University, Wuhan 430079, People's Republic of China

⁷ Central South University, Changsha 410083, People's Republic of China

⁸ China Center of Advanced Science and Technology, Beijing 100190, People's Republic of China

⁹ COMSATS University Islamabad, Lahore Campus, Defence Road, Off Raiwind Road, 54000 Lahore, Pakistan

¹⁰ Fudan University, Shanghai 200433, People's Republic of China

¹¹ G.I. Budker Institute of Nuclear Physics SB RAS (BINP), Novosibirsk 630090, Russia

¹² GSI Helmholtzcentre for Heavy Ion Research GmbH, D-64291 Darmstadt, Germany

¹³ Guangxi Normal University, Guilin 541004, People's Republic of China

¹⁴ Guangxi University, Nanning 530004, People's Republic of China

¹⁵ Hangzhou Normal University, Hangzhou 310036, People's Republic of China

¹⁶ Hebei University, Baoding 071002, People's Republic of China

¹⁷ Helmholtz Institute Mainz, Staudinger Weg 18, D-55099 Mainz, Germany

¹⁸ Henan Normal University, Xinxiang 453007, People's Republic of China

¹⁹ Henan University of Science and Technology, Luoyang 471003, People's Republic of China

²⁰ Henan University of Technology, Zhengzhou 450001, People's Republic of China

²¹ Huangshan College, Huangshan 245000, People's Republic of China

²² Hunan Normal University, Changsha 410081, People's Republic of China

²³ Hunan University, Changsha 410082, People's Republic of China

²⁴ Indian Institute of Technology Madras, Chennai 600036, India

²⁵ Indiana University, Bloomington, Indiana 47405, USA

²⁶ INFN Laboratori Nazionali di Frascati, (A)INFN Laboratori Nazionali di Frascati, I-00044, Frascati, Italy; (B)INFN Sezione di Perugia, I-06100, Perugia, Italy; (C)University of Perugia, I-06100, Perugia, Italy

²⁷ INFN Sezione di Ferrara, (A)INFN Sezione di Ferrara, I-44122, Ferrara, Italy;

Ferrara, Italy; (B)University of Ferrara, I-44122, Ferrara, Italy

²⁸ Institute of Modern Physics, Lanzhou 730000, People's Republic of China

²⁹ Institute of Physics and Technology, Peace Ave. 54B, Ulaanbaatar 13330, Mongolia

³⁰ Jilin University, Changchun 130012, People's Republic of China

³¹ Johannes Gutenberg University of Mainz, Johann-Joachim-Becher-Weg 45, D-55099 Mainz, Germany

³² Joint Institute for Nuclear Research, 141980 Dubna, Moscow region, Russia

³³ Justus-Liebig-Universitaet Giessen, II. Physikalisches Institut, Heinrich-Buff-Ring 16, D-35392 Giessen, Germany

³⁴ Lanzhou University, Lanzhou 730000, People's Republic of China

³⁵ Liaoning Normal University, Dalian 116029, People's Republic of China

³⁶ Liaoning University, Shenyang 110036, People's Republic of China

³⁷ Nanjing Normal University, Nanjing 210023, People's Republic of China

³⁸ Nanjing University, Nanjing 210093, People's Republic of China

³⁹ Nankai University, Tianjin 300071, People's Republic of China

⁴⁰ National Centre for Nuclear Research, Warsaw 02-093, Poland

⁴¹ North China Electric Power University, Beijing 102206, People's Republic of China

⁴² Peking University, Beijing 100871, People's Republic of China

⁴³ Qufu Normal University, Qufu 273165, People's Republic of China

⁴⁴ Shandong Normal University, Jinan 250014, People's Republic of China

⁴⁵ Shandong University, Jinan 250100, People's Republic of China

⁴⁶ Shanghai Jiao Tong University, Shanghai 200240, People's Republic of China

⁴⁷ Shanxi Normal University, Linfen 041004, People's Republic of China

⁴⁸ Shanxi University, Taiyuan 030006, People's Republic of China

⁴⁹ Sichuan University, Chengdu 610064, People's Republic of China

⁵⁰ Soochow University, Suzhou 215006, People's Republic of China

⁵¹ South China Normal University, Guangzhou 510006, People's Republic of China

⁵² Southeast University, Nanjing 211100, People's Republic of China

⁵³ State Key Laboratory of Particle Detection and Electronics, Beijing 100049, Hefei 230026, People's Republic of China

- ⁵⁴ Sun Yat-Sen University, Guangzhou 510275, People's Republic of China
⁵⁵ Suranaree University of Technology, University Avenue 111, Nakhon Ratchasima 30000, Thailand
⁵⁶ Tsinghua University, Beijing 100084, People's Republic of China
⁵⁷ Turkish Accelerator Center Particle Factory Group, (A)Istinye University, 34010, Istanbul, Turkey; (B)Near East University, Nicosia, North Cyprus, Mersin 10, Turkey
⁵⁸ University of Chinese Academy of Sciences, Beijing 100049, People's Republic of China
⁵⁹ University of Groningen, NL-9747 AA Groningen, The Netherlands
⁶⁰ University of Hawaii, Honolulu, Hawaii 96822, USA
⁶¹ University of Jinan, Jinan 250022, People's Republic of China
⁶² University of Manchester, Oxford Road, Manchester, M13 9PL, United Kingdom
⁶³ University of Muenster, Wilhelm-Klemm-Str. 9, 48149 Muenster, Germany
⁶⁴ University of Oxford, Keble Rd, Oxford, UK OX13RH
⁶⁵ University of Science and Technology Liaoning, Anshan 114051, People's Republic of China
⁶⁶ University of Science and Technology of China, Hefei 230026, People's Republic of China
⁶⁷ University of South China, Hengyang 421001, People's Republic of China
⁶⁸ University of the Punjab, Lahore-54590, Pakistan
⁶⁹ University of Turin and INFN, (A)University of Turin, I-10125, Turin, Italy; (B)University of Eastern Piedmont, I-15121, Alessandria, Italy; (C)INFN, I-10125, Turin, Italy
⁷⁰ Uppsala University, Box 516, SE-75120 Uppsala, Sweden
⁷¹ Wuhan University, Wuhan 430072, People's Republic of China
⁷² Xinyang Normal University, Xinyang 464000, People's Republic of China
⁷³ Yunnan University, Kunming 650500, People's Republic of China
⁷⁴ Zhejiang University, Hangzhou 310027, People's Republic of China
⁷⁵ Zhengzhou University, Zhengzhou 450001, People's Republic of China
- ^a Also at the Moscow Institute of Physics and Technology, Moscow 141700, Russia
^b Also at the Novosibirsk State University, Novosibirsk, 630090, Russia
^c Also at the NRC "Kurchatov Institute", PNPI, 188300, Gatchina, Russia
^d Also at Goethe University Frankfurt, 60323 Frankfurt am Main, Germany
- ^e Also at Key Laboratory for Particle Physics, Astrophysics and Cosmology, Ministry of Education; Shanghai Key Laboratory for Particle Physics and Cosmology; Institute of Nuclear and Particle Physics, Shanghai 200240, People's Republic of China
- ^f Also at Key Laboratory of Nuclear Physics and Ion-beam Application (MOE) and Institute of Modern Physics, Fudan University, Shanghai 200443, People's Republic of China
- ^g Also at State Key Laboratory of Nuclear Physics and Technology, Peking University, Beijing 100871, People's Republic of China
- ^h Also at School of Physics and Electronics, Hunan University, Changsha 410082, China
- ⁱ Also at Guangdong Provincial Key Laboratory of Nuclear Science, Institute of Quantum Matter, South China Normal University, Guangzhou 510006, China
- ^j Also at Frontiers Science Center for Rare Isotopes, Lanzhou University, Lanzhou 730000, People's Republic of China
- ^k Also at Lanzhou Center for Theoretical Physics, Lanzhou University, Lanzhou 730000, People's Republic of China
- ^l Also at the Department of Mathematical Sciences, IBA, Karachi, Pakistan

The study of the Cabibbo-favored semileptonic decay $\Lambda_c^+ \rightarrow \Lambda e^+ \nu_e$ is reported using a 4.5 fb^{-1} data sample of $e^+ e^-$ annihilations collected at center-of-mass energies ranging from 4.600 GeV to 4.699 GeV with the BESIII detector at the BEPCII collider. The branching fraction of the decay is measured to be $\mathcal{B}(\Lambda_c^+ \rightarrow \Lambda e^+ \nu_e) = (3.56 \pm 0.11_{\text{stat.}} \pm 0.07_{\text{syst.}})\%$, which is the most precise measurement to date. Furthermore, we perform an investigation of the internal dynamics in $\Lambda_c^+ \rightarrow \Lambda e^+ \nu_e$. We provide the first direct comparisons of the differential decay rate and form factors with those predicted from lattice quantum chromodynamics (LQCD) calculations. Combining the measured branching fraction with a q^2 -integrated rate predicted by LQCD, we determine $|V_{cs}| = 0.936 \pm 0.017_{\mathcal{B}} \pm 0.024_{\text{LQCD}} \pm 0.007_{\tau_{\Lambda_c}}$.

The study of Λ_c^+ semileptonic (SL) decays provides valuable information about weak and strong interactions in baryons containing a heavy quark ¹. Measurement of the SL decay rate of the Λ_c^+ can help elucidate the role of nonperturbative effects in strong interactions [1]. In particular, the Cabibbo-favored (CF) SL decay $\Lambda_c^+ \rightarrow \Lambda \ell^+ \nu_\ell$

($\ell = e, \mu$), which is the dominant component in Λ_c^+ SL decays [2], is the most interesting to measure. Its decay rate depends on the weak quark mixing Cabibbo-Kobayashi-Maskawa (CKM) matrix [3] element $|V_{cs}|$ and strong interaction effects parameterized by form factors describing the hadronic transition between the initial and the final baryons. Measurement of $|V_{cs}|$ via $\Lambda_c^+ \rightarrow \Lambda \ell^+ \nu_\ell$ is an important consistency test for the standard model (SM) and a probe for new physics beyond the SM [1, 4], complementary to D meson analyses.

¹ Throughout this Letter, charge-conjugate modes are implied unless explicitly noted.

In recent years, significant progress has been achieved in the study of Λ_c^+ SL decays, both experimentally [5–7] and theoretically [8–25]. In 2015, the BESIII collaboration reported the first measurement of the absolute branching fraction (BF) for $\Lambda_c^+ \rightarrow \Lambda e^+ \nu_e$ with $\mathcal{B}(\Lambda_c^+ \rightarrow \Lambda e^+ \nu_e) = (3.63 \pm 0.38_{\text{stat.}} \pm 0.20_{\text{syst.}})\%$ [5]. The absolute BF for $\Lambda_c^+ \rightarrow \Lambda \mu^+ \nu_\mu$ [7] was reported later. These BESIII measurements motivated the first LQCD calculation on the CF SL decay $\Lambda_c^+ \rightarrow \Lambda \ell^+ \nu_\ell$ in 2017, with a predicted BF $\mathcal{B}(\Lambda_c^+ \rightarrow \Lambda e^+ \nu_e) = (3.80 \pm 0.19_{\text{LQCD}} \pm 0.11_{\tau_{\Lambda_c^+}})\%$ [14] which is consistent with the BESIII result. Reference [14] also investigated the internal dynamics and predicted the form factors and differential decay rates in $\Lambda_c^+ \rightarrow \Lambda e^+ \nu_e$ decay. This was followed by a series of other LQCD calculations [22–25] in this sector. This theoretical work is important for understanding the decay mechanism in SL decays in the charmed baryon sector. However, there is no direct experimental data for testing and calibrating calculations of differential decay rates and form factors. Experimental studies of the dynamics in $\Lambda_c^+ \rightarrow \Lambda e^+ \nu_e$ can provide these information.

In this Letter, we report an improved measurement of the absolute BF of $\Lambda_c^+ \rightarrow \Lambda e^+ \nu_e$ using data sets collected at the BESIII at the center-of-mass energies $\sqrt{s} = 4.600, 4.612, 4.628, 4.641, 4.661, 4.682$, and 4.699 GeV. The total integrated luminosity for these data samples is 4.5 fb^{-1} [26, 27], which includes and is about 7 times larger than that used in Ref. [5]. Furthermore, for the first time, we measure the differential decay rate and form factors in $\Lambda_c^+ \rightarrow \Lambda e^+ \nu_e$ and provide the direct comparisons with those predicted by the LQCD calculations [14].

Details about the BESIII detector design and performance are provided in Ref. [28]. A GEANT4-based [29] Monte Carlo (MC) detector simulation is used to determine signal detection efficiencies and to estimate potential backgrounds. Signal MC samples of $e^+e^- \rightarrow \Lambda_c^+ \bar{\Lambda}_c^-$ with one Λ_c^+ baryon decaying to $\Lambda e^+ \nu_e$ together with a $\bar{\Lambda}_c^-$ decaying to the hadronic decay mode used for this analysis are generated by KKMC [30] with EVTGEN [31]. This includes initial-state radiation [32] and final-state radiation [33] effects. The signal MC sample of the SL decay $\Lambda_c^+ \rightarrow \Lambda e^+ \nu_e$ is generated using the form factors measured in this work. To study the backgrounds, an inclusive MC sample consisting of open-charm states, radiative return to charmonium(like) ψ states at lower masses, and continuum processes of $q\bar{q}$ ($q = u, d$, and s), along with Bhabha scattering, $\mu^+\mu^-, \tau^+\tau^-$, and $\gamma\gamma$ events are generated. All known decay modes of open-charm and ψ states are simulated using BFs specified by the Particle Data Group (PDG) [2], while the remaining unknown ψ decays are modeled with LUNDCHARM [34, 35].

We select the “single-tag” (ST) and “double-tag” (DT) samples as described in Refs. [5, 7]. STs are $\bar{\Lambda}_c^-$ baryons reconstructed from their daughter particles in one of four-

teen hadronic decays as used in Ref. [36]. DTs are events with a ST and a Λ_c^+ baryon reconstructed as $\Lambda e^+ \nu_e$. The ST $\bar{\Lambda}_c^-$ signals are identified using the beam constrained mass:

$$M_{\text{BC}} = \sqrt{(\sqrt{s}/2)^2 - |\vec{p}_{\bar{\Lambda}_c^-}|^2},$$

where $\vec{p}_{\bar{\Lambda}_c^-}$ is the measured momentum of the ST $\bar{\Lambda}_c^-$. A kinematic variable $\Delta E = E_{\text{beam}} - E_{\bar{\Lambda}_c^-}$ is required to improve the signal significance for ST $\bar{\Lambda}_c^-$ baryons. If an event satisfies more than one $\bar{\Lambda}_c^-$ tags, only the tag with the minimum $|\Delta E|$ is kept to avoid the double counting among STs with the same final state. The ΔE requirements, M_{BC} distributions and their ST yields are documented in Ref. [36]. The total ST yield reconstructed with fourteen ST modes is $N_{\text{ST}} = 122\,268 \pm 474$, where the uncertainty is calculated by the weighted average according to the fit results of each tag mode.

Candidates for $\Lambda_c^+ \rightarrow \Lambda e^+ \nu_e$ are selected from the remaining tracks recoiling against the ST $\bar{\Lambda}_c^-$ candidates in the signal mass window. To select the Λ , the same criteria as those used in the ST selection are applied [36]. Detection and reconstruction of the positron follow the procedures in Ref. [5]. As the neutrino is not detected, we employ the kinematic variable $U_{\text{miss}} = E_{\text{miss}} - c|\vec{p}_{\text{miss}}|$ to obtain information on the neutrino, where E_{miss} and \vec{p}_{miss} are the missing energy and momentum carried by the neutrino, respectively, and are defined in the same way as in Ref. [5]. Figure 1 (left) shows the distribution of $M_{p\pi^-}$ versus U_{miss} for the $\Lambda_c^+ \rightarrow \Lambda e^+ \nu_e$ candidates in data. A cluster of the events is located around the intersection of the Λ mass and $\Lambda e^+ \nu_e$ signal region near $U_{\text{miss}} \simeq 0$. Requiring $M_{p\pi^-}$ to be within the Λ signal region, we project the distribution onto the U_{miss} axis, as shown in Fig. 1(right). To obtain the number of signal events, the U_{miss} distribution is fitted with a signal function f which consists of a Gaussian to describe the core of the U_{miss} distribution and two power-law tails to account for initial and final state radiations [5, 37]. Two MC-simulated background shapes are used to describe the peaking backgrounds from $\Lambda_c^+ \rightarrow \Lambda \pi^+ \pi^0$ and $\Lambda_c^+ \rightarrow \Lambda \mu^+ \nu_\mu$, and a MC-simulated non-resonant background shape is used to describe the continuous background. From the fit, we obtain the yield of $\Lambda_c^+ \rightarrow \Lambda e^+ \nu_e$ decay $N^{\text{DT}} = 1253 \pm 39$, where the uncertainty is statistical only.

The absolute BF for $\Lambda_c^+ \rightarrow \Lambda e^+ \nu_e$ is determined by

$$\mathcal{B}(\Lambda_c^+ \rightarrow \Lambda e^+ \nu_e) = \frac{N^{\text{DT}}}{N^{\text{ST}} \times \varepsilon_{\text{semi}}}, \quad (1)$$

where $\varepsilon_{\text{semi}} = (\sum_{ij} N_{ij}^{\text{ST}} \times \epsilon_{ij}^{\text{DT}} / \epsilon_{ij}^{\text{ST}}) / N^{\text{ST}} = 0.2876$ is the average efficiency for detecting the $\Lambda_c^+ \rightarrow \Lambda e^+ \nu_e$ decay in ST events [5], and i and j represent the ST modes and the data samples at different center-of-mass energies, respectively. The parameters N_{ij}^{ST} , $\epsilon_{ij}^{\text{ST}}$ and $\epsilon_{ij}^{\text{DT}}$ are the

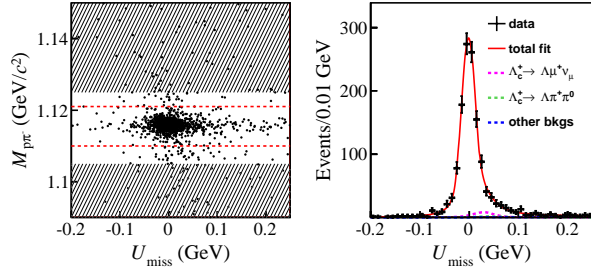


FIG. 1. (left) The $M_{p\pi^-}$ versus U_{miss} distribution for the $\Lambda_c^+ \rightarrow \Lambda e^+ \nu_e$ candidates. The area between the dashed lines denotes the Λ signal region and the hatched areas indicate the Λ sideband regions. (right) Projected U_{miss} distribution within the Λ signal region together with the fit.

ST yields, ST and DT efficiencies, respectively. Inserting the values of N^{DT} , N^{ST} , and ϵ_{semi} in Eq. (1), we measure $\mathcal{B}(\Lambda_c^+ \rightarrow \Lambda e^+ \nu_e) = (3.56 \pm 0.11 \pm 0.07)\%$, where the first uncertainty is statistical, and the second is systematic as described below.

With the DT technique, the BF measurements are insensitive to the systematic uncertainties of the ST selection. The remaining systematic uncertainties in the BF measurement are now described. The uncertainties of the e^+ tracking and particle identification (PID) efficiencies are determined to be 0.4% and 0.5% using radiative Bhabha events. The uncertainty due to Λ reconstruction is determined to be 0.2%, using $J/\psi \rightarrow pK^-\bar{\Lambda}$ and $J/\psi \rightarrow \Lambda\bar{\Lambda}$ control samples. The uncertainty associated with the simulation of the SL signal model is estimated to be 0.6% by varying the input form-factor parameters, determined in this work, by one standard deviation. The ST yield (1.0%) is evaluated by using alternative signal shapes in fits to the M_{BC} spectra. We also considered the following systematic uncertainties: fit to the U_{miss} distribution (1.0%) estimated by using alternative signal shapes and background shapes, the quoted BF for $\Lambda \rightarrow p\pi^-$ (0.8%), and the MC statistics (0.8%). Adding these contributions in quadrature gives a total systematic uncertainty of 2.0% for the $\mathcal{B}(\Lambda_c^+ \rightarrow \Lambda e^+ \nu_e)$ measurement.

The differential decay rate of $\Lambda_c^+ \rightarrow \Lambda e^+ \nu_e$ can be expressed using four variables: $e^+\nu_e$ mass-squared (q^2), the angle between the proton momentum in the Λ rest frame and the Λ momentum in the Λ_c rest frame (θ_p), the angle between the positron momentum in the decay of $W^+ \rightarrow e^+\nu_e$ rest frame and the Λ momentum in the Λ_c rest frame (θ_e), and the acoplanarity angle between the Λ and W^+ decay planes (χ). It can be described in

terms of helicity amplitudes $H_{\lambda\Lambda\lambda_W}$ by [38–40]:

$$\begin{aligned} \frac{d^4\Gamma}{dq^2 d\cos\theta_e d\cos\theta_p d\chi} &= \frac{G_F^2 |V_{cs}|^2}{2(2\pi)^4} \cdot \frac{P q^2}{24 M_{\Lambda_c}^2} \times \\ &\left\{ \frac{3}{8} (1 - \cos\theta_e)^2 |H_{\frac{1}{2}1}|^2 (1 + \alpha_\Lambda \cos\theta_p) \right. \\ &+ \frac{3}{8} (1 + \cos\theta_e)^2 |H_{-\frac{1}{2}-1}|^2 (1 - \alpha_\Lambda \cos\theta_p) \\ &+ \frac{3}{4} \sin^2\theta_e [|H_{\frac{1}{2}0}|^2 (1 + \alpha_\Lambda \cos\theta_p) + |H_{-\frac{1}{2}0}|^2 (1 - \alpha_\Lambda \cos\theta_p)] \\ &+ \frac{3}{2\sqrt{2}} \alpha_\Lambda \cos\chi \sin\theta_e \sin\theta_p \times \\ &\left. [(1 - \cos\theta_e) H_{-\frac{1}{2}0} H_{\frac{1}{2}1} + (1 + \cos\theta_e) H_{\frac{1}{2}0} H_{-\frac{1}{2}-1}] \right\} \quad (2) \end{aligned}$$

where $H_{\lambda\Lambda\lambda_W} = H_{\lambda\Lambda\lambda_W}^V - H_{\lambda\Lambda\lambda_W}^A$ and $H_{-\lambda\Lambda-\lambda_W}^{V(A)} = (+/-)H_{\lambda\Lambda\lambda_W}^{V(A)}$, G_F is the Fermi coupling constant, $|V_{cs}| = 0.97320 \pm 0.00011$ [2] is a CKM matrix element, P is the magnitude of the Λ momentum in the Λ_c rest frame, M_{Λ_c} is the mass of Λ_c [2], and α_Λ is the $\Lambda \rightarrow p\pi^-$ decay asymmetry parameter [2].

The helicity amplitudes parameterized in Eq. (2) are related to four form factors by [14]:

$$\begin{aligned} H_{\frac{1}{2}1}^V &= \sqrt{2Q_-} f_{\perp}(q^2), \quad H_{\frac{1}{2}1}^A = \sqrt{2Q_+} g_{\perp}(q^2), \\ H_{\frac{1}{2}0}^V &= \sqrt{Q_-/q^2} f_+(q^2) (M_{\Lambda_c} + M_\Lambda), \\ H_{\frac{1}{2}0}^A &= \sqrt{Q_+/q^2} g_+(q^2) (M_{\Lambda_c} - M_\Lambda), \end{aligned} \quad (3)$$

where $Q_\pm = (M_{\Lambda_c} \pm M_\Lambda)^2 - q^2$ and M_Λ is the Λ mass [2]. The form factors $f_{\perp,+}(q^2)$ and $g_{\perp,+}(q^2)$ are defined following a z -expansion of the parameters as in Ref. [14]:

$$f(q^2) = \frac{a_0^f}{1 - q^2 / (m_{\text{pole}}^f)^2} \left[1 + \alpha_1^f \times z(q^2) \right], \quad (4)$$

where m_{pole}^f is the pole mass; a_0^f , α_1^f are free parameters; $z(q^2) = \frac{(\sqrt{t_+ - q^2} - \sqrt{t_+ - t_0})}{(\sqrt{t_+ - q^2} + \sqrt{t_+ - t_0})}$ with $t_0 = q_{\max}^2 = (m_{\Lambda_c} - m_\Lambda)^2$, $t_+ = (m_D + m_K)^2$, $m_D = 1.870 \text{ GeV}/c^2$ and $m_K = 0.494 \text{ GeV}/c^2$. The pole masses are $m_{\text{pole}}^{f_{\perp}, f_{\perp}} = 2.112 \text{ GeV}/c^2$ and $m_{\text{pole}}^{g_{\perp}, g_{\perp}} = 2.460 \text{ GeV}/c^2$ [14].

For these four form factors, the amplitudes at $q^2 = 0$ are denoted as $a_0^{f_{\perp}}$, $a_0^{f_+}$, $a_0^{g_{\perp}}$, and $a_0^{g_+}$, respectively. As the differential decay rate defined in Eq. (2) has to be normalized, we can only determine the ratios of these amplitudes and α_1^f in the maximum likelihood (ML) fit. Here, we choose $a_0^{g_{\perp}}$ as the reference since the terms with form factor parameters $a_0^{g_{\perp,+}}$ are dominant compared with that of $a_0^{f_{\perp,+}}$ in the $\Lambda_c^+ \rightarrow \Lambda e^+ \nu_e$ decay. Furthermore, we set $\alpha_1^{g_{\perp}} \equiv \alpha_1^{g_+}$ and $\alpha_1^{f_{\perp}} \equiv \alpha_1^{f_+}$ taking into account that the kinematic dependences of $g_{\perp}(q^2)$ and $g_+(q^2)$, $f_{\perp}(q^2)$ and $f_+(q^2)$ as a function of q^2 are similar according to the LQCD calculation [14]. Hence, there are five independent free parameters in the ML fit for the

differential decay amplitude: $\alpha_1^{g\perp}$, $\alpha_1^{f\perp}$, $r_{f+} = a_0^{f+}/a_0^{g\perp}$, $r_{f\perp} = a_0^{f\perp}/a_0^{g\perp}$, and $r_{g+} = a_0^{g+}/a_0^{g\perp}$.

A four-dimensional ML fit is performed as a function of q^2 , $\cos\theta_e$, $\cos\theta_p$, and χ for $\Lambda_c^+ \rightarrow \Lambda e^+ \nu_e$ events within $-0.06 < U_{\text{miss}} < 0.06$ GeV. The projections of the fit onto q^2 , $\cos\theta_e$, $\cos\theta_p$, and χ are shown in Fig. 2. The fit procedure is validated using large inclusive MC samples, and the pull distribution of each fitted parameter is consistent with a normal distribution. The fitted form-factor parameters of $\alpha_1^{g\perp}$, $\alpha_1^{f\perp}$, r_{f+} , $r_{f\perp}$, r_{g+} are given in Table I. The goodness of fit is estimated by using the χ^2/ndof with a similar method as applied in Ref. [41], where ndof denotes the number of degrees of freedom. The χ^2 is calculated from the comparison between the measured and expected number of events in the four-dimensional space of the kinematic variables q^2 , $\cos\theta_e$, $\cos\theta_p$, and χ which are initially divided into 2, 3, 3, and 3 bins, respectively. The χ^2/ndof is evaluated to be 0.85. The systematic uncertainties arise mainly from the uncertainties related to positron tracking and PID efficiencies, Λ reconstruction efficiency, the background normalization and the Λ decay parameter. The systematic uncertainties arising from the requirements placed on the positron and the Λ are estimated by varying the positron tracking and PID efficiencies, and Λ reconstruction efficiency by $\pm 0.4\%$, $\pm 0.5\%$ and $\pm 0.2\%$, respectively. The systematic uncertainty because of the background normalization is estimated by varying its value by $\pm 13\%$ which take into account the uncertainty of the background estimations. The systematic uncertainty in α_Λ is evaluated by varying its nominal value by $\pm 1\sigma$. All of the variations mentioned above will result in differences of the fitted parameters from that under the nominal conditions. These differences are assigned as the systematic uncertainties and summarized in Table II, where the total systematic uncertainty is obtained by adding all contributions in quadrature.

In order to determine the parameter of $a_0^{g\perp}$, the differential decay rate is related to $\mathcal{B}(\Lambda_c^+ \rightarrow \Lambda e^+ \nu_e)$ measured in this work and the lifetime of Λ_c (τ_{Λ_c}) by:

$$\int_0^{q_{\max}^2} \frac{d\Gamma}{dq^2} dq^2 = \frac{\mathcal{B}(\Lambda_c^+ \rightarrow \Lambda e^+ \nu_e)}{\tau_{\Lambda_c}}, \quad (5)$$

where $d\Gamma/dq^2$ is the integration of the differential decay rate given in Eq. (2) over the other three kinematic variables and expressed as:

$$\frac{d\Gamma}{dq^2} = \frac{G_F^2 |V_{cs}|^2}{192\pi^3 M_{\Lambda_c}^2} \times P q^2 \times \left[|H_{\frac{1}{2}1}|^2 + |H_{-\frac{1}{2}-1}|^2 + |H_{\frac{1}{2}0}|^2 + |H_{-\frac{1}{2}0}|^2 \right]. \quad (6)$$

Inserting $\tau_{\Lambda_c} = 202.4 \pm 3.1$ fs [2], the CKM element $|V_{cs}| = 0.97320 \pm 0.00011$ [2] and the helicity amplitudes

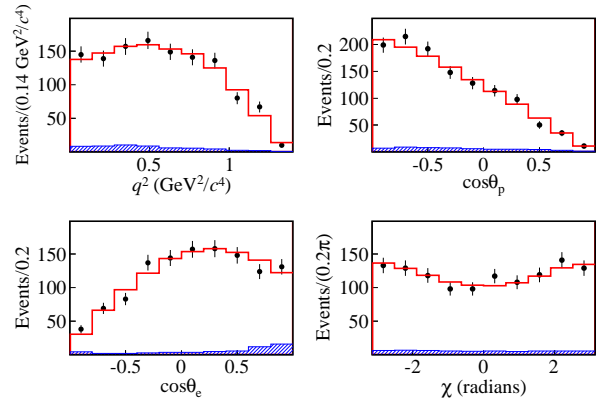


FIG. 2. Projections of the fitted kinematic variables, comparing data (dots with error bars) and MC. Solid and shadowed histograms are the MC-simulated signal plus background and the MC-simulated background.

parameterized with form factors as in Eq. (3), we determine $a_0^{g\perp} = 0.54 \pm 0.04_{\text{stat.}} \pm 0.01_{\text{syst.}}$

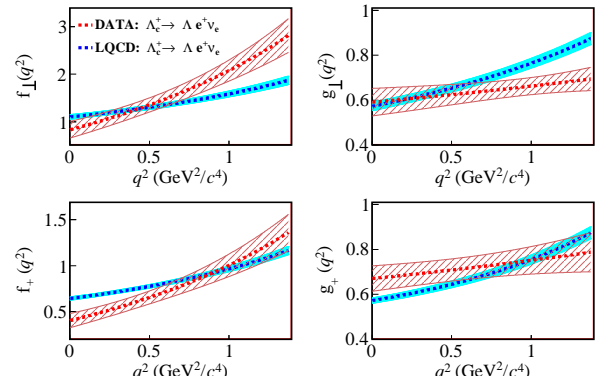


FIG. 3. Comparison of form factors with LQCD calculations. The bands show the total uncertainties.

With the measured parameters and their correlation coefficients shown in Table I, we obtain the dependences of form factors of $f_\perp(q^2)$, $f_+(q^2)$, $g_\perp(q^2)$, and $g_+(q^2)$, and the differential decay rate as a function of q^2 in the SL decay $\Lambda_c^+ \rightarrow \Lambda e^+ \nu_e$. Figures 3 and 4 show comparisons of the FFs and the differential decay rate between measurements in this work and that in LQCD calculations. Results of LQCD calculations are obtained using the nominal values listed in Table IV in Ref. [14]. We note that the dependences of measured FFs show different kinematic behavior compared to those predicted from LQCD calculations. In particular, discrepancies can be seen at high q^2 regions for $f_\perp(q^2)$ and $g_\perp(q^2)$, as well as at low q^2 regions for $f_+(q^2)$. For $f_+(q^2)$ and $f_\perp(q^2)$, our measurement tends to have steeper slope than those from LQCD calculations, while on the contrary for $g_+(q^2)$

TABLE I. Measured form-factor parameters, where the first errors are statistical and the second are systematic. The lower table shows the correlation coefficients of statistical and systematic uncertainties between the form factor parameters.

Parameters	$\alpha_1^{g_\perp}$	$\alpha_1^{f_\perp}$	r_{f+}	r_{f_\perp}	r_{g+}
Values	$1.43 \pm 2.09 \pm 0.16$	$-8.15 \pm 1.58 \pm 0.05$	$1.75 \pm 0.32 \pm 0.01$	$3.62 \pm 0.65 \pm 0.02$	$1.13 \pm 0.13 \pm 0.01$
Coefficients	$\alpha_1^{g_\perp}$	$\alpha_1^{f_\perp}$	r_{f+}	r_{f_\perp}	r_{g+}
$a_0^{g_\perp}$	-0.64	0.60	-0.66	-0.83	-0.40
$\alpha_1^{g_\perp}$		-0.63	0.62	0.53	-0.33
$\alpha_1^{f_\perp}$			-0.79	-0.67	-0.07
r_{f+}				0.57	-0.09
r_{f_\perp}					0.39

TABLE II. Systematic uncertainties (in %) of the fitted parameters.

Parameter	Tracking&PID& Λ	Normalization	α_Λ	Total
$a_1^{f_\perp}$	0.6	0.5	0.1	0.8
$a_1^{g_\perp}$	6.0	7.2	2.8	9.8
r_{f+}	0.1	0.5	0.7	0.9
r_{g_\perp}	0.3	0.1	0.6	0.7
r_{g+}	0.3	1.5	0.1	1.5

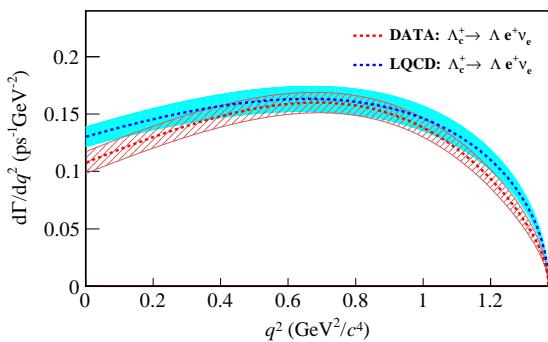


FIG. 4. Comparison of the differential decay rates with LQCD predictions. The band show the total uncertainties.

and $g_\perp(q^2)$. The corresponding comparison on differential decay rates, shown in Fig. 4, gives fair agreement throughout the q^2 region.

In summary, we report an improved measurement of the absolute BF for $\Lambda_c^+ \rightarrow \Lambda e^+ \nu_e$, $\mathcal{B}(\Lambda_c^+ \rightarrow \Lambda e^+ \nu_e) = (3.56 \pm 0.11 \pm 0.07)\%$, based on 4.5 fb^{-1} of data collected at center-of-mass energies ranging from 4.600 GeV to 4.699 GeV with BESIII. This work supersedes our previous measurement [5] and improves the precision of the world average value more than threefold. Comparisons of the BF from this work and theoretical predictions are shown in Table III. The predicted BFs in Refs. [8–12] differ by more than two standard deviations with respect to

TABLE III. Comparison of $\mathcal{B}(\Lambda_c^+ \rightarrow \Lambda e^+ \nu_e)$ from theoretical calculations and our measurement.

	$\mathcal{B}(\Lambda_c^+ \rightarrow \Lambda e^+ \nu_e) [\%]$
Constituent quark model (HONR) [8]	4.25
Light-front approach [9]	1.63
Covariant quark model [10]	2.78
Relativistic quark model [11]	3.25
Non-relativistic quark model [12]	3.84
Light-cone sum rule [13]	3.0 ± 0.3
Lattice QCD [14]	3.80 ± 0.22
$SU(3)$ [15]	3.6 ± 0.4
Light-front constituent quark model [16]	3.36 ± 0.87
MIT bag model [16]	3.48
Light-front quark model [17]	4.04 ± 0.75
This work	$3.56 \pm 0.11 \pm 0.07$

the mean value of our measured $\mathcal{B}(\Lambda_c^+ \rightarrow \Lambda e^+ \nu_e)$. Thus, our measurement disfavors these predictions at a confidence level of more than 95%. Combing $\mathcal{B}(\Lambda_c^+ \rightarrow \Lambda e^+ \nu_e)$ measured in this work, τ_{Λ_c} and the q^2 -integrated rate predicted by LQCD [14], we determine $|V_{cs}| = 0.936 \pm 0.017_B \pm 0.024_{\text{LQCD}} \pm 0.007_{\tau_{\Lambda_c}}$, which is in consistent with $|V_{cs}| = 0.939 \pm 0.038$ measured in $D \rightarrow K \ell \nu_\ell$ decays [2] within one standard deviation.

Furthermore, by analyzing the dynamics of $\Lambda_c^+ \rightarrow \Lambda e^+ \nu_e$, we measure the $\Lambda_c^+ \rightarrow \Lambda$ decay form factors for the first time. Our results provide the first direct comparisons on the differential decay rates and form factors with those obtained from LQCD calculations. Currently, the statistical uncertainty dominates in the total uncertainty of our result and the measurement can be improved with more experimental data available in the future [42]. The comparisons of differential decay rate and form factors between experimental measurements and LQCD predictions presented in this work provide important inputs in understanding the SL decays of charmed baryons. Our results will also help calibrate the calculation of SL decays of other charmed baryons [43, 44] as well as the Λ_b [17–19, 24, 45–48].

We thank Wei Wang for useful discussions on the differential decay rate of $\Lambda_c^+ \rightarrow \Lambda e^+ \nu_e$. The BESIII col-

laboration thanks the staff of BEPCII and the IHEP computing center for their strong support. This work is supported in part by National Key R&D Program of China under Contracts Nos. 2020YFA0406400, 2020YFA0406300; National Natural Science Foundation of China (NSFC) under Contracts Nos. 11635010, 11735014, 11835012, 11935015, 11935016, 11935018, 11961141012, 12022510, 12025502, 12035009, 12035013, 12192260, 12192261, 12192262, 12192263, 12192264, 12192265; the Chinese Academy of Sciences (CAS) Large-Scale Scientific Facility Program; Joint Large-Scale Scientific Facility Funds of the NSFC and CAS under Contract No. U1832207; CAS Key Research Program of Frontier Sciences under Contract No. QYZDJ-SSW-SLH040; 100 Talents Program of CAS; INPAC and Shanghai Key Laboratory for Particle Physics and Cosmology; ERC under Contract No. 758462; European Union's Horizon 2020 research and innovation programme under Marie Skłodowska-Curie grant agreement under Contract No. 894790; German Research Foundation DFG under Contracts Nos. 443159800, Collaborative Research Center CRC 1044, GRK 2149; Istituto Nazionale di Fisica Nucleare, Italy; Ministry of Development of Turkey under Contract No. DPT2006K-120470; National Science and Technology fund; STFC (United Kingdom); The Royal Society, UK under Contracts Nos. DH140054, DH160214; The Swedish Research Council; U.S. Department of Energy under Contract No. DE-FG02-05ER41374.

-
- [1] J. D. Richman and P. R. Burchat, *Rev. Mod. Phys.* **67**, 893 (1995).
 - [2] P.A. Zyla *et al.* (Particle Data Group), *Prog. Theor. Exp. Phys.* **2020**, 083C01 (2020) and 2021 update.
 - [3] M. Kobayashi and T. Maskawa, *Prog. Theor. Phys.* **49**, 652 (1973).
 - [4] S. Aoki *et al.*, *Eur. Phys. J. C* **80**, 113 (2020).
 - [5] M. Ablikim *et al.* [BESIII Collaboration], *Phys. Rev. Lett.* **115**, 221805 (2015).
 - [6] M. Ablikim *et al.* [BESIII Collaboration], *Phys. Rev. Lett.* **121**, 251801 (2018).
 - [7] M. Ablikim *et al.* [BESIII Collaboration], *Phys. Lett. B* **767**, 42 (2017).
 - [8] M. Pervin, W. Roberts and S. Capstick, *Phys. Rev. C* **72**, 035201 (2005).
 - [9] Z. X. Zhao, *Chin. Phys. C* **42**, 093101 (2018).
 - [10] T. Gutsche, M. A. Ivanov, J.G. Körner, V. E. Lyubovitskij and P. Santorelli, *Phys. Rev. D* **93**, 034008 (2016).
 - [11] R. N. Faustov, V. O. Galkin, *Eur. Phys. J. C* **76** 628 (2016).
 - [12] M. M. Hussain and W. Roberts, *Phys. Rev. D* **95**, 053005 (2017); *Phys. Rev. D* **95**, 099901(E) (2017).
 - [13] Y. L. Liu, M. Q. Huang and D. W. Wang, *Phys. Rev. D* **80**, 074011 (2009).
 - [14] S. Meinel, *Phys. Rev. Lett.* **118**, 082001 (2017).
 - [15] C. Q. Geng, C. W. Liu, and T. H. Tsai, S. W. Yeh, *Phys. Lett. B* **792**, 214 (2019).
 - [16] C. Q. Geng, Chong-Chung Lih, C. W. Liu, and T. H. Tsai, *Phys. Rev. D* **101**, 094017 (2020).
 - [17] Y. S. Li, X. Liu and F. S. Yu, *Phys. Rev. D* **104**, 013005 (2021).
 - [18] K. Azizi, M. Bayar, Y. Sarac and H. Sundu, *Phys. Rev. D* **80**, 096007 (2009).
 - [19] T. Gutsche, M. A. Ivanov, J.G. Körner, V. E. Lyubovitskij and P. Santorelli, *Phys. Rev. D* **90**, 114033 (2014); *Phys. Rev. D* **94**, 059902(E) (2016).
 - [20] N. Ikeno, and E. Oset, *Phys. Rev. D* **93**, 014021 (2016).
 - [21] C. D. Lü, W. Wang, F. S. Yu, *Phys. Rev. D* **93**, 056008 (2016).
 - [22] S. Meinel, *Phys. Rev. D* **97**, 034511 (2018).
 - [23] S. Meinel and G. Rendon, *Phys. Rev. D* **105**, L051505 (2022).
 - [24] S. Meinel and G. Rendon, *Phys. Rev. D* **105**, 054511 (2022).
 - [25] H. Bahtiyar, *Turk. J. Phys.* **45**, 185 (2021).
 - [26] M. Ablikim *et al.* [BESIII Collaboration], *Chin. Phys. C* **39**, 093001 (2015).
 - [27] M. Ablikim *et al.* [BESIII Collaboration], arXiv:2205.04809.
 - [28] M. Ablikim *et al.* [BESIII Collaboration], *Nucl. Instrum. Meth. A* **614**, 345 (2010).
 - [29] S. Agostinelli *et al.* [GEANT4 Collaboration], *Nucl. Instrum. Meth. A* **506**, 250 (2003).
 - [30] S. Jadach, B. F. L. Ward and Z. Was, *Comput. Phys. Commun.* **130**, 260 (2000); *Phys. Rev. D* **63**, 113009 (2001).
 - [31] D. J. Lange, *Nucl. Instrum. Meth. A* **462**, 152 (2001); R. G. Ping, *Chin. Phys. C* **32**, 599 (2008).
 - [32] E. A. Kurav and V. S. Fadin, *Sov. J. Nucl. Phys.* **41**, 466 (1985).
 - [33] E. Richter-Was, *Phys. Lett. B* **303**, 163 (1993).
 - [34] J. C. Chen, G. S. Huang, X. R. Qi, D. H. Zhang and Y. S. Zhu, *Phys. Rev. D* **62**, 034003 (2000).
 - [35] Yang Rui-Ling, Ping Rong-Gang and Chen Hong, *Chin. Phys. Lett.* **31** 061301 (2014).
 - [36] M. Ablikim *et al.* [BESIII Collaboration], arXiv:2207.11483.
 - [37] J. Y. Ge *et al.* [CLEO Collaboration], *Phys. Rev. D* **79**, 052010 (2009).
 - [38] J.G. Körner and M. Krämer, *Phys. Lett. B* **275**, 495 (1992).
 - [39] CLEO Collaboration, J.W. Hinson, *et al.*, *Phys. Rev. Lett.* **94**, 191801 (2005).
 - [40] A. Kadeer, Körner and U. Moosbrugger, *Eur. Phys. J. C* **59**, 27 (2009).
 - [41] M. Ablikim *et al.* [BESIII Collaboration], *Phys. Rev. D* **99**, 011103R (2019).
 - [42] M. Ablikim *et al.* [BESIII Collaboration], *Chin. Phys. C* **44**, 040001 (2020).
 - [43] Q. A. Zhang, H. Hua, F. Huang, R. Li, Y. Li, C. D. Lü, P. Sun, W. Wang and Y. B. Yang, *Chin. Phys. C* **46**, 011002 (2022).
 - [44] X. G. He, F. Huang, W. Wang, Z. P. Xing, *Phys. Lett. B* **823**, 136765 (2021).
 - [45] T. Feldmann and M. W. Y. Yip, *Phys. Rev. D* **85**, 014035 (2012); *Phys. Rev. D* **86**, 079901(E) (2012).
 - [46] W. Detmold, C. J. David Lin, S. Meinel and M. Wingate, *Phys. Rev. D* **88**, 014512 (2013).
 - [47] W. Detmold, C. Lehner, and S. Meinel, *Phys. Rev. D* **92**,

034503 (2015).

[48] W. Detmold and S. Meinel, *Phys. Rev. D* **93**, 074501 (2016).